Research Article

Developmental Dynamics
DOI 10.1002/dvdy.24610

Avian embryonic coronary arterio-venous pattering involves the contribution of different endothelial and endocardial cell populations

Paul Palmquist-Gomes[1,2], Juan Antonio Guadix[1,2*], José M. Pérez-Pomares[1,2*]

1. Department of Animal Biology, Faculty of Sciences, University of Málaga, Instituto Malagueño de Biomedicina (IBIMA), Campus de Teatinos s/n, 29080 Málaga, Spain.

2. BIONAND, Centro Andaluz de Nanomedicina y Biotecnología (Junta de Andalucía, Universidad de Málaga), c/ Severo Ochoa nº25, 29590 Campanillas, Málaga, Spain.

***Correspondence to:** José M. Pérez-Pomares, PhD. Department of Animal Biology. Faculty of Science. Campus de Teatinos s/n. Málaga 29071. SPAIN. Tel: +34 952-136-653; Fax: +34 952-131-668; E-mail: jmperezp@uma.es or Juan A. Guadix Domínguez, PhD. Department of Animal Biology. Faculty of Science. Campus de Teatinos s/n. Málaga 29071. SPAIN. Tel: +34 952-367-621; Fax: +34 952-131-668; E-mail: jaguadix@uma.es.

Running title: Avian coronary arterio-venous origins.

Keywords: Heart; Coronary arteries; Coronary veins; Distal cardiac outflow tract; Proepicardium.

Key findings:

- Avian coronary endothelium forms from at least 3 different embryonic endothelial/endocardial cell populations.
- Avian ventricular endocardium and distal cardiac outflow tract-derived endothelial cells are significant contributors to coronary endothelium.
- Both angiogenesis and vasculogenesis are active during early coronary vessel formation.
- Different coronary domains are preferentially contributed by defined populations of endothelial cells.
- Prospective coronary and veins remain disconnected during the first phases of coronary blood vessel formation.

Grant sponsor & number: Spanish Ministry of Economy (MINECO) grants BFU2015-65783-R and SAF2015-71863 (to JMPP); Instituto de Salud Carlos III (MINECO-ISCIII) grant RD16/0011/0030-TERCEL (to JMPP); Plan Propio-Universidad de Málaga (to JAG).

Received: Jul 21, 2017; Revised: Nov 13, 2017; Accepted: Dec 05, 2017

Abstract

Background: Coronary vasculature irrigates the myocardium and is crucial to late embryonic and adult heart function. Despite the developmental significance and clinical relevance of these blood vessels, the embryonic origin and the cellular and molecular mechanisms that regulate coronary arterio-venous patterning are not known in detail. In this study, we have used the avian embryo to dissect the ontogenetic origin and morphogenesis of coronary vasculature. **Results:** We show that sinus venosus endocardial sprouts and proepicardial angioblasts pioneer coronary vascular formation, invading the developing heart simultaneously. We also report that avian ventricular endocardium has the potential to contribute to coronary vessels, and describe the incorporation of cardiac distal outflow tract endothelial cells to the peritruncal endothelial plexus to participate in coronary vascular formation. Finally, our findings indicate that large sinus venosus-independent sections of the forming coronary vasculature develop without connection to the systemic circulation and that coronary arterio-venous shunts form a few hours before peritruncal arterial endothelium connects to the aortic root. **Conclusions:** Embryonic coronary vasculature is a developmental mosaic, formed by the integration of vascular cells from, at least, four different embryological origins, which assemble in a coordinated manner to complete coronary vascular development.

Introduction

The coronary vascular system is a complex network of arteries, capillaries and veins that supports blood circulation in the cardiac chamber walls, guaranteeing proper heart performance. Accordingly, congenital anomalies of coronary vessels may alter coronary circulation and thus have an impact on postnatal and adult life (Pérez-Pomares et al., 2016). Despite the extreme pathophysiological importance of coronary blood vessels, fundamental aspects of their embryogenesis remain unknown.

The embryonic origin of the coronary endothelial cells has been extensively discussed (Rychter & Oštádal, 1971; Viragh & Challice, 1981; Hirakow, 1983; Conte & Pellegrini, 1984; Hutchins et al., 1988; Mikawa & Fischman, 1992; Poelmann et al., 1993; Vrancken Peeters et al., 1997a,b; Pérez-Pomares et al., 1998; Männer, 1999). Although none of the previous studies primarily intended to establish a single origin for coronary endothelium, it is frequent to find these and other works quoted to support the hypothesis of embryonic coronary intimal layer being formed from one endothelial population only (Red-Horse et al., 2010; Tian et al., 2015). Recent research, however, has crucially suggested that the embryonic coronary endothelium may derive from multiple cellular sources (Katz et al., 2012; Wu et al., 2012; Cano et al., 2016; Théveniau-Ruissy et al., 2016; Zhang et al., 2016).

Our current interpretation of coronary embryonic development is strongly influenced by the combined analysis and extrapolation of results from studies carried out in different animal models. Retroviral tagging experiments and chimeric quail-to-chick transplantations unambiguously indicate that a significant part of the avian coronary vascular system is a proepicardium (PE) derivative (Mikawa & Fischman, 1992; Pérez-Pomares et al., 1998; Männer, 1999; Guadix et al., 2006; Nesbitt et al., 2006; Pérez-Pomares et al., 2002a,b), but no experimental data are available in the literature on the endocardial contribution to avian coronary endothelium. On the contrary, genetic tracing in the mouse embryo confirms an extensive contribution of sinus venosus (Zhang et al., 2016), ventricular endocardium (Wu et al., 2012) and the PE to coronary endothelium (Cano et al., 2016).

In this study, we have taken advantage of the unique characteristics of the avian embryo, a classic model for the study of coronary vascular development, to assess the ability of different endothelial/endocardial populations to contribute to coronary endothelium and to study the developmental mechanics of coronary vascular morphogenesis. We would like to suggest that the hypothesis of coronary endothelium being a developmental mosaic better explains coronary vascular complexity, including the developmental dynamics of the assembly of coronary arteries and veins in the developing ventricular walls. In this regard, previous research on mouse coronary development suggests that coronary arteries are genetically reprogrammed from prospective coronary veins formed the sinus venosus endocardium (Red-Horse et al., 2010), while other studies claim that a significant part of coronary endothelium derives from ventricular endocardium (Wu et al., 2012). Since murine prospective coronary veins are known to be located subepicardially and major arteries intramyocardially (Wagner et al., 2005; Lavine & Ornitz, 2008; Red-Horse et al., 2010; Cano et al., 2016), the first study (Red-Horse et al.,

2010) implies the existence of a signal gradient directing primitive coronary endothelial growth from the surface of the heart towards the ventricular lumen (Tian et al., 2013). On the contrary, the assumption that ventricular endocardium is a major contributor to coronary endothelium (Wu et al., 2012) would require endocardial cell migration from the cardiac lumen to the subepicardium (Pires-Gomes & Pérez-Pomares, 2013). In the present work, we reconcile all these views with the anatomical evidence of prospective coronary arteries being isolated from the systemic blood flow during a significant period of time (Waldo et al., 1990; Ando et al., 2004; Ivins et al., 2015; Théveniau-Ruissy et al., 2016).

Results

Sinus venosus endocardium sprouts and proepicardial angioblasts grow simultaneously into the developing heart

Fluorescein-conjugated *Lens culinaris* lectin (LC-FITC) injection in quail embryos (Fig.1A-C) allowed for the identification of the embryonic vasculature supporting active blood circulation (QH1 antibody was used as a general counterstain for quail endothelium). LC-FITC injections prior to PE attachment to the heart surface (HH16-17, 60 hours of incubation, Fig.1D, E) show that the endocardium is the only vascular tissue present in the heart chamber walls (Fig.1E). LC-FITC injections 24 hours after PE attachment to the myocardial surface (HH21, 80 hours of incubation, Fig.1F, G), reveal that LC-FITC^{+} sinus venosus endocardial sprouts are growing subepicardially towards the atrioventricular and ventricular myocardium (Fig.1G); some the more distal cells in these structures show a tip-like morphology (Fig.1G'). The presence of LC-FITC in the proximal part of these vascular sprouts (QH1^{+}/LC-FITC^{+}) confirms they have a lumen and are connected to the systemic circulation (Fig.1G, G'). Large amounts of QH1^{+}/LC-FITC^{-} vascular endothelial cells invade the subepicardial space together with SV endocardium-derived vessels (Fig.1G). Late LC-FITC injections (HH26, 120 hours of incubation) still identify endocardial sprouts projecting towards the subepicardium (Fig.1H); the majority of non-perfused developing vascular structures (QH1^{+}/LC-FITC^{-}) form at a deeper level, embedded in the myocardial wall (Fig.1H). As we proceeded from the cardiac inflow (Fig.1I-L) towards the ventricular apex (Fig.1M-P), a unique distribution of primitive coronary vessels is observed. Vascular structures forming in close vicinity of the sinus venosus (HH23) always display a vascular lumen, are LC-FITC^{+}, and do not invade the ventricular myocardium (Fig.1I-L). Primitive coronary vessels forming in the ventricular walls segregate in two different domains: QH1^{+}/LC-FITC^{+} developing coronary vessels remain in the subepicardial space (Fig.1O, P), while angioblasts and some other QH1^{+}/LC-FITC^{-} vascular structures locate intramyocardially (Fig.1N, P). At later stages (HH28-29, 6.5 days of incubation), this characteristic location of LC-FITC^{+} and LC-FITC^{-} primitive coronary vascular structures persists (Fig.1Q-T).

Primitive coronary vasculature is comprised of two different but overlapping endothelial networks

To better understand the complex topology of the developing coronary vasculature, we submitted LC-FITC-injected quail embryos (Fig.1A-C) to QH1 whole mount immunohistochemistry and studied the arrangement of blood-perfused ($QH1^+/LC\text{-}FITC^+$) versus non blood-perfused vascular sections ($QH1^+/LC\text{-}FITC^-$). At HH23 (4.5 incubation days), blood-perfused ($QH1^+/LC\text{-}FITC^+$) sinus venosus endocardium sprouts locate at the surface of the heart, being more frequently found in the dorsal ventricular wall (Fig.2A, A', B). Some $QH1^+/LC\text{-}FITC^-$ isolated cells (putative coronary angioblasts) distribute close to these dorsal $QH1^+/LC\text{-}FITC^+$ vessels (Fig.2B). Large numbers of $QH1^+/LC\text{-}FITC^-$ isolated cells were also found around $QH1^+/LC\text{-}FITC^+$ vessels, in the dorsal (Fig.2A) and ventral (Fig.2C) ventricular walls. Some of these $QH1^+/LC\text{-}FITC^-$ cells coalesce to form vasculogenic chords (Fig.2A', C'). Just before the embryonic coronary arterial capillary plexus connects to the aortic root (HH28-29, 6.5 incubation days), superficial $QH1^+/LC\text{-}FITC^+$ vessels are found covering the dorsal atrioventricular myocardium and most of the dorsal ventricular wall (Fig.2D, E). Connection between $QH1^+/LC\text{-}FITC^+$ sinus venosus-derived vessels and $QH1^+/LC\text{-}FITC^-$ vessels starts to be frequent; some of these vascular shunts are $LC\text{-}FITC^+$ while some other remain $LC\text{-}FITC^-$ (Fig.2E). On the cardiac ventral wall, the proportion of $LC\text{-}FITC^+$ (blood-perfused vessels) has increased around the atrioventricular canal. These vessels have not fully extended towards the ventricular wall and apex (Fig.2F). To study the patterning of developing coronary vascular structures from a different perspective, atrial chambers and the distal parts of the aortic and pulmonary trunks of HH29 embryos were removed. QH1/LC-FITC-stained hearts were photographed from the cardiac base (Fig.2G-J). The analysis of these whole mount samples shows that different $QH1^+/LC\text{-}FITC^+$ and $QH1^+/LC\text{-}FITC^-$ prospective coronary vascular networks develop together at the dorsal cardiac surface. The peritruncal capillary plexus, which is mostly $QH1^+/LC\text{-}FITC^-$, surrounds the base of the forming pulmonary and aortic trunks, also extending distally (Fig.2G-N). Both the more distal periarterial vascular plexus (Fig.2K, L, M) and the peritruncal capillary plexus (Fig.2K, N) do not show extensive connections with the coronary vasculature developing on the dorsal cardiac surface.

Chimeric PE tracing shows stage-dependent plasticity of proepicardial angioblasts

Since LC-FITC staining is not able to identify the ontogenetic origin of endothelial cells, we constructed quail-to-chick PE chimeras (Fig. 3A) and then injected them with LC-FITC before fixation (Fig.3A', A''). This experiment allows for the simultaneous tracing of PE-derived endothelial cells and the identification of their status with respect to the systemic circulation (only LC-FITC+ endothelium is connected to the systemic flow). All samples were counterstained with LC-FITC prior to the connection of prospective coronary arteries to the aortic root (around 7 days of incubation, HH30). At HH23-24, $QH1^+$ cells at the cardiac inflow either associate to $LC\text{-}FITC^+$ endothelium of subepicardial vascular structures (Fig. 3B) or integrate as part of this same endothelium (Fig. 3C). As we move apically, $QH1^+/LC\text{-}FITC^-$ cells

are found scattered on the surface of the ventricles (Fig. 3D). Around 24 hours later (HH26), many QH1$^+$/LC-FITC$^+$ donor-derived cells are identified in the subepicardial vessels, while only a few intramyocardial QH1$^+$ cells could be recorded at this time (Fig. 3E). At HH28-29, QH1+ most cells remain forming part of the intimal layer of subepicardial LC-FITC$^+$ coronary vessels (Fig. 3F), although some other QH1$^+$ cells are found deep in the myocardium forming small, primitive vascular structures which are not connected to the systemic circulation (LC-FITC$^-$) (Fig. 3F, G). Whole-mount stainings of LC-FITC injected HH28-29 quail-to-chick proepicardial chimeras confirm these data (Fig.H-I').

Three days after coronary arterial plexus connection to the aortic root (HH42), only arterial endothelium displays *EPHRINB2* and *NOTCH1* gene expression (Fig. 3J-M'). In our chimeras, donor endothelial cells were found in both prospective venous and non-venous endothelial domains of the chimeric embryos. Some of these cells integrate in the endothelium of mature arterial sections, as shown by the co-localization of the donor vascular marker (QH1) and arterial endothelium-specific EphrinB2 (Fig. 3J, K') and Notch1 mRNA transcripts (Fig. 3L, M'). Quantitation of donor (QH1$^+$) PE-derived endothelial contribution to developing coronary blood vessels prior to the connection of arterial vessels to the aortic root (HH28-29) indicates that only 29.15±5.66% of such cells contribute to the prospective venous endothelium (LC-FITC$^+$). The rest of QH1$^+$ cells incorporate in the intramyocardial prospective arterial and capillary vascular networks.

Proepicardial and ventricular quail-to-chick chimeras

Recent studies on the origin of murine coronary endothelium have suggested that the ventricular endocardium, migrating from the inner to the outer cardiac surface, contributes to coronary endothelium (Wu et al., 2012). We thus aimed to test the coronary potential of avian ventricular endocardium using quail-to-chick chimeras in combination with intravascular LC-FITC injections (Fig.4). As compared to proepicardial chimeras (Fig. 4A-G), quail ventricular transplantation onto chick hearts (Fig. 4H-N) reveals that the majority of early donor endocardial cells incorporate to the host endocardium after transplantation (HH23, Fig. 4I-K). At later stages (HH28-29), many donor endocardial cells locate in the host endocardium, but some of them form coronary-like structures in the outer, ventricular compact layer (Fig. 4L-N).

Distal outflow tract quail-to-chick chimeras

The abundance of QH1+ endothelial cells found in the walls of the developing cardiac outflow tract of quail embryos prompted us to check whether endothelial cells at the arterial pole of the heart contribute to coronary vascular development. In order to do so, the upper distal outflow tract of HH18-19 embryos was either labelled with DiO (chick) or homotopically transplanted (quail) to HH17-18 chick hosts (Fig.5A). After 3 days of incubation, the aortic and pulmonary roots were inspected (Fig. 5B). Only the upper, distal part of the cardiac outflow tract was found to be stained in control embryos (Fig. 5C, D, E). After 48 hours of incubation, the DiO stain concentrates in the truncal myocardium (Fig.6F, G). VEGFR2$^+$ angioblasts and endothelial

cells are abundant in the floor of the aortic sac (Fig.5F, G) and the cardiac outflow tract walls; some of these VEGFR2^{+} cells were also DiO^{+} (Fig. 5G, H, H'). To confirm the incorporation of cardiac distal outflow tract cells to the forming peritruncal capillary plexus (Fig. 5J), homotopic chimeric transplantation of quail distal outflow tract tissue to chick embryo hosts was performed. The results of this experiment confirm the incorporation of donor-derived distal cardiac outflow tract QH1+ endothelial cells to the pulmonary and aortic roots (Fig. 5K-L).

A summary of the experimental methods used to trace the fate of coronary endothelial cells and the results provided by each method is included in Table 1.

Discussion

Research on cardiac vascularization by coronary endothelium has proven to be challenging due to various reasons. The first one is the reduced number of molecular tools available for the identification and tracking of specific endothelial subpopulations (Pérez-Pomares et al., 2016). An additional difficulty that limits the sequential analysis of endothelial progenitor/cell growth, coalescence and fusion is that the differentiation of endothelial cells from angioblast progenitors and their assembly to form primitive vascular structures occurs rapidly (Flamme et al., 1995; Drake et al., 1997; Drake & Fleming, 2000). Furthermore, endothelial progenitors and early embryonic endothelial cells show high plasticity, differentiating into particular cell phenotypes (e.g. arterial or venous) in response to changing environmental cues (Moyon et al., 2001; le Noble et al., 2004).

In accordance to all these limitations, the identification of the origin of coronary endothelium has been submitted to controversy for decades (Red-Horse et al., 2010; Wu et al., 2012; Tian et al., 2015; Pérez-Pomares et al., 2016). Careful analysis of recent publications in the field reveals that such controversy is often based in the assumption that all coronary endothelium derives from a single endothelial cell progenitor pool (discussed in Zhang & Pu, 2013; Tian et al., 2015; Pérez-Pomares et al., 2016). Such interpretation relies in results derived from *in vivo*, Cre/LoxP-based cell lineage tracing of murine coronary endothelium (Zhou & Pu, 2012; Wu et al., 2012; Cano et al., 2016). Cre/LoxP is a powerful genetic technology that does not, however, allow for the discrimination of multiple, independent cell lineages as based on the expression of a single molecular marker (Zhou & Pu, 2012). Hence, contradictory conclusions on the development of coronary blood vessels may reflect the restricted ability of the Cre-LoxP technology to study the quantitative dynamics of more than one endothelial cell population at the time, as well as to provide information on the functional status of different coronary vasculature domains. Relevant to this discussion, it has been suggested that the quantitative contribution of different endocardial/endothelial cells to vertebrate coronary endothelium needs to be regarded carefully, as a relatively small population of endothelial cells could be key to the completion of specific segments of the coronary vascular circuitry (Cano et al., 2016).

In order to integrate, complete and complement published data on the origin of coronary endothelium and the developmental dynamics of coronary morphogenesis, we have revisited coronary blood vessel formation in the avian embryo, a classical model for the study of

cardiovascular embryonic development (Mikawa & Fischman, 1992; Poelmann et al., 1993; Mikawa & Gourdie, 1996; Dettman et al., 1998; Pérez-Pomares et al., 1998; Männer, 1999). As opposed to the mouse embryo, the chick one allows for the combined use of several experimental techniques to obtain new data and improve our understanding coronary blood vessel development.

Our results show that endothelial/endocardial cells from different sources (sinus venosus endocardium, ventricular endocardium, PE and distal cardiac outflow tract mesenchyme) independently contribute to the formation of embryonic coronary vasculature. This conclusion is based in the following findings. First, intravascular LC-FITC injections at different developmental stages allowed us to distinguish between two subsets of primitive coronary blood vessels. One of them corresponds to sinus venosus dorsal endocardial sprouts (starting around the third incubation day), which were first described by Lewis more than a century ago (Lewis, 1904). These sprouts are polarized, contain a vascular lumen from their inception and are soon perfused by blood, as shown by their fast incorporation of LC-FITC. Since adult coronary veins drain into the coronary sinus, which is a partial derivative of the embryonic sinus venosus (Steding et al., 1990), we think these primitive embryonic vessels represent a developmental scaffold for the formation of coronary veins. These LC-FITC+ sinus venosus endocardial sprouts progressively encircle the atrioventricular groove, growing from the dorsal cardiac wall towards the ventral one. Some studies pointed to VEGF as the major chemotactic signal guiding coronary vessel growth (Tomanek et al., 2006; Liu et al., 2010; Tomanek et al., 2010), we thus used a modified fibrin matrix bound to VEGF (Ruiz-Villalba et al., 2013) to show that these primitive coronary endothelial cells at the venous cardiac pole indeed migrate in response to VEGF, efficiently invading the recombinant fibrin matrix. This finding also suggests that sinus venosus endocardium outgrowth is an active, developmentally patterned process (Red-Horse et al., 2010).

Sinus venosus endocardial sprouts, however, are not the only endothelial cells invading the heart at these stages. Previous studies have shown that multiple QH1+ angioblasts (endothelial progenitors) migrate from the PE to reach the atrioventricular and ventricular myocardium via the subepicardium (Kattan et al., 2004). Our results prove that, starting at incubation day 4 (HH23), some of these angioblasts assemble and form subepicardial primitive cord-like vascular structures which remain disconnected from the systemic blood flow (LC-FITC$^-$) for at least three days. This latter feature suggests that such primitive vascular structures are not directly related with sinus venosus endocardial sprouts since these are, as we have previously shown, connected to the systemic circulation from the very moment of their formation. Later in development, vascular structures disconnected from the systemic circulation (not perfused by blood, LC-FITC) also form in the depth of the ventricular walls, while sinus venosus endocardium-derived blood vessels (LC-FITC$^+$, connected to systemic blood flow) remain confined to the subepicardial space. All these results confirm that both angiogenic and vasculogenic blood vessel growth mechanisms are active during the early phases of coronary development (Pérez-Pomares et al., 1998; Kattan et al., 2004; Red-Horse et al., 2010). Another

conclusion that can be drawn from our LC-FITC injections is that the embryonic vascular sections disconnected from the systemic circulation, including the peritruncal capillary plexus at the base of the cardiac outflow tract, are unlikely to be ontogenetically related to sinus venosus endocardium. This is in agreement with pioneer studies on coronary vascular development, which identified these peritruncal endothelial cells as the origin of left and right coronary arterial stem endothelium (Bogers et al., 1989; Waldo et al., 1990; Ando et al., 2004;) and described them forming a plexus of vascular structures disconnected from the systemic flow (Waldo et al., 1990).

To evaluate the contribution of PE angioblasts to avian coronary development, we took advantage of interspecific quail-to-chick transplantations and combined them with intravascular LC-FITC injections. Together, these two techniques become a powerful tool to study PE contribution to coronary vasculature. Our results show that proepicardial endothelial derivatives in early (HH23) PE quail-to-chick chimeras associate and/or incorporate to the nascent coronary vasculature, which at these stages is basically comprised of blood-perfused LC-FITC^{+} sinus venosus endocardium-derived vessels (prospective coronary veins). Later on (HH26-29), PE angioblasts are also found to contribute to LC-FITC^{-} blood vessel segments, most especially in the ventricular walls. These findings might suggest that avian PE angioblasts significantly contribute to coronary endothelium during the early phases of coronary vascular development, but also that these endothelial cells, like extraembryonic ones (le Noble et al., 2004), are not originally committed to a venous or an arterial fate. Surprisingly, donor-derived endothelial cells (QH1^{+}) in late chimeras (HH42) are more frequent in arterial (EphrinB2^{+}/Notch1^{+}) than in venous coronary endothelial domains (EphrinB2^{-}/Notch1^{-}), but it is not clear whether this is a consequence of primitive coronary endothelium remodelling or a time-dependent, developmentally-regulated restriction of proepicardial-derived endothelial fate. Unfortunately, the restricted availability of bona fide markers for avian venous endothelium prevents us from characterizing this phase of avian coronary development in more detail.

In addition to sinus venosus endocardium and proepicardial angioblasts, studies in the mouse embryo have identified the ventricular endocardium as a third, relevant source of coronary endothelium (Wu et al., 2012; Zhang & Zhou, 2013). However, it is not known whether avian ventricular endocardium also participates in coronary vascular formation. To retrieve information on the coronary potential of ventricular endocardium, we grafted pieces of quail ventricles (H16-17) onto the cardiac surface of chick host embryos (HH16-17). Results from this experiment reveal that the majority of donor ventricular endocardial cells in early chimeras (HH23) migrate towards the cardiac lumen to mix with the host ventricular endocardium against the predicted endocardial-to-epicardial direction path. In later chimeras (HH28), donor-derived endocardium also displays a similar trend, but is also able to give rise to vascular structures in the outer ventricular wall. These findings demonstrate that avian ventricular endocardium has the potential to contribute to coronary endothelium, but it remains unclear whether the incorporation of ventricular endocardial cells to the forming coronary vessels is a passive phenomenon, depending on the complex events that take place during ventricular wall

trabeculation and maturation (Grego-Bessa et al., 2007; Luxán et al., 2013), or rather an active endothelial growth guided by chemotactic cues provided by adjacent tissues.

As it can be inferred from the previous discussion, at least three different types of endothelia/endocardial cells contribute to the formation of primitive avian coronary endothelium: sinus venosus endocardium, ventricular endocardium and PE angioblasts. To further evaluate whether endothelial cells from the arterial pole of the heart could also be recruited to the developing coronary endothelium as recently suggested (Théveniau-Ruissy et al., 2016), we performed quail-to-chick distal outflow tract tissue homotopic transplantations. The analysis of this new type of chimeras reveals a significant, distal to proximal incorporation of endothelial cells to the peritruncal capillary plexus, i.e. the embryonic coronary domain that will eventually connect with the aortic lumen to form the right and left coronary arterial stems (Waldo et al., 1990). Although the chemotactic signals that guide this migration are not know, the CXCL12-CXCR4 axis, reported to be involved in the formation of coronary artery stems from peritruncal endothelial cells (Ivins et al., 2015), stands as a potential candidate. Since the donor grafts included cells from the subpharyngeal mesenchyme and the aortic sac endothelium, it is not possible to ascertain whether cardiac arterial pole-derived endothelial cells directly derive from the aortic sac endothelium or differentiate from the anterior/second secondary heart field (Kelly et al., 2001; Waldo et al., 2001). These results, which were further confirmed by DiO *in vivo* cell tracking experiments, identify a novel origin for at least part of peritruncal (prospective arterial) endothelial cells in the tissues surrounding the distal part of the cardiac outflow tract.

The careful inspection of previously reported results on coronary embryonic development (Mikawa et al., 1992; Pérez-Pomares et al., 1998, 2002; Katz et al., 2012; Cano et al., 2016) suggests there are intrinsic differences in coronary morphogenesis between avians (chick and quail) and mammals (mouse). The most significant discrepancies between these species relate to the relative contribution of different endothelial sources to coronary blood vessel formation and the final location of large coronary arterial tracts in these vertebrate models. Regarding the origins of coronary endothelial cells, it has been shown elsewhere that extracardiac (proepicardial) endothelial contribution to coronary formation is quite extensive, while studies in mouse embryos restrict the proepicardial contribution to a rough 20% of coronary endothelial cells. We believe that the characteristic, early attachment of the avian proepicardium to the atrioventricular myocardium can explain this difference, as the avian proepicardium becomes a permanent path for the fast and continuous migration of extracardiac endothelial cells to the surface of the heart at the time of coronary morphogenesis. On the other hand, the definitive location of large coronary arterial vessels is also different in both animal models. While major coronary arteries run intramyocardially in mice, large avian coronary vessels are mostly subepicardial (Pérez-Pomares et al., 2016). We think that avian coronary artery formation is likely to involve an early subepicardial confinement of prospective coronary arterial endothelial cells, followed by a rapid stabilization of large arteries through the formation of their medial wall. On the contrary, we hypothesize that the depletion of coronary arterial endothelium throughout the ventricular wall is a more progressive event in the mouse embryo,

explaining the preferential intramyocardial location of major coronary arteries in this species. It is also possible that differential expression of chemotactic cues involved in coronary vascular formation occurs between mouse and avian embryos, but further research is necessary to confirm this point.

In summary, our work indicates that the developing avian coronary vasculature recruits endothelial cells from the sinus venosus endocardium as well as from extracardiac sources at the venous (PE) and arterial (distal cardiac outflow tract) poles of the heart. PE and distal cardiac outflow tract-derived endothelial cells display significantly different behaviours, as PE endothelial cells incorporate to both prospective venous and arterial endothelium while distal cardiac outflow tract endothelial cells preferentially join to the peritruncal coronary arterial endothelium. Moreover, we have confirmed the coronary vascular potential of ventricular endocardium. Although our work does not exclude a possible transdifferentiation of venous endothelial cells into arterial ones (Red-Horse et al., 2010), it clearly shows that the early coronary vasculature is an ontogenetically heterogeneous group of blood vessels requiring the contribution of various endothelial cell populations (Fig.6m). Then, we also report that only a part of the vascular networks that form during early coronary development are connected to the systemic blood flow. Such primitive coronary blood vessels grow independently from other segments of the developing vasculature which are not connected to systemic blood circulation. These two types of primitive coronary vascular networks seem to assemble just before prospective coronary arteries connect to the aortic root, i.e. before a complete coronary blood circuitry is established (Pérez-Pomares et al., 2016). Our work provides new data on the cellular mechanisms that participate in normal coronary blood vessel development, and might help us to increase our understanding of the etiology of coronary congenital anomalies.

Experimental Procedures

Quail and chick embryos

The animals used in our research program were handled in compliance with the international guidelines (1964 Declaration of Helsinki) for animal care and welfare. Experimental procedures have been revised and approved by the Ethics Committee at the University of Málaga. Eggs were kept in a rocking incubator at 38ºC. Embryos were staged according to the Hamburger and Hamilton stages of chick development (Hamburger & Hamilton, 1951). Routine tissue inspection of the samples was performed using hematoxylin-eosin staining.

Lens culinaris *(LC) lectin injections*

Around 1µl of undiluted FITC-conjugated *Lens culinaris* agglutinin (VECTOR FL1041) was microinjected into the embryonic vasculature of avian embryos via vitelline veins (HH17-26) or allantoic veins (HH29) (Jilani et al., 2003). Injected embryos were re-incubated for 10

minutes, excised and fixed in 4%PFA overnight/4ºC and processed for immunohistochemistry as described. At least 10 embryos were injected per each stage.

Quail to chick chimeras

Quail donor embryos were incubated until stages HH16-17, excised, and washed in sterile PBS. For proepicardial transplantations (15 chimeras), quail proepicardia were carefully dissected using tungsten needles, small iridectomy forceps and scissors and transplanted into prospective pericardial cavity, close to the inner curvature of HH16-17 (60 hours of incubation) chick embryo host hearts. For the endocardial chimeras (7 chimeras), HH16-17 quail ventricles were isolated and opened in sterile PBS, and then grafted into the prospective pericardial cavity with the quail endocardium facing to the chick myocardium of HH16-17 chick embryos. Some PE and ventricular chimeras were injected with LC-FITC 2 days (HH23-24) and 4 days (HH29) after surgery. Distal cardiac outflow tract chimeras (6 chimeras) were constructed homotopically grafting small quail tissue pieces from the upper distal outflow tract of HH18-19 quail embryos into HH17-18 chick hosts. All chimeras were typically fixed 24-48 hours after transplantation. I all cases embryos were isolated, washed in PBS and fixed in PFA (4%) overnight at 4ºC. Samples were dehydrated in a graded series of ethanol, cleared in butanol, embedded in Paraplast (56ºC), sectioned (10μm) and mounted on microscope slides (MENZEL-GLÄSER). The relative PE-derived endothelial cell contribution to prospective venous versus non-venous ventricular domains was calculated as the percentage of $QH1^{+}$/$LC\text{-}FITC^{+}$ cells with respect to the total number of QH1+ cells ($QH1^{+}$/$LC\text{-}FITC^{+}$ & $QH1^{+}$/$LC\text{-}FITC^{-}$) using the IMARIS software. In total, four HH28-29 chimeras were inspected and counts were carried out in 5 histological sections per chimera (the minimal distance between sections was 50μm).

DiO cell tracking

To trace cardiac arterial pole endothelial cells, 3,3′-Dioctadecyloxacarbocyanine perchlorate (DiO, SIGMA D1554) *in vivo* cell stainings were carried out in eight chick embryos. In detail, a micromanipulator (Narishige) was used to hold a single DiO crystal next to the uppermost part of the distal outflow tract of HH18-19 chick embryos for 45 seconds. Then the DiO was removed, the eggs sealed with Scotch tape, and reincubated for 48 hours. Embryos were fixed in 1%PFA, cryopreserved in sucrose (15-30%), embedded in OCT resin (TissueTek) and sectioned in a cryostat (10μm).

Immunohistochemistry

Immunohistochemical characterization of donor-derived chimeric tissues was performed using the QH1 antibody, a known quail endothelial cell marker. Single QH1 immunofluorescence on tissue sections was performed by blocking non-specific binding sites with SBT and incubating the slides in the primary QH1 antibody (1/100 diluted, DSHB) overnight at 4ºC. Then, the slides were washed in TPBS solution (3x5 minutes) and incubated for 2 hours at room temperature in Cy5 AffiniPure Donkey Anti-Mouse IgG (1/200 diluted, Jackson 715-175-

150). Double QH1-cTnT immunofluorescence on sections was performed with the same protocol previously described, using QH1 (1/100 diluted, DSHB) and cardiac troponin cTnT1 (1/100 diluted, Santa Cruz 15368) as primary antibodies. Alexa Fluor® 647 AffiniPure Donkey Anti-Rabbit IgG (1/200 diluted, Jackson 711-605-152) and TRITC-conjugated Goat Anti-Mouse IgG (1/200 diluted, Sigma T5393) were used as secondary antibodies. Optional nuclear DAPI (1/2000 diluted, Sigma D9542) counterstaining was performed. Finally, the slides were mounted and analyzed under a LEICA SP5 laser confocal microscope.

For whole-mount QH1 staining, whole hearts were isolated in PBS and fixed in PFA (4%) overnight at 4ºC. Samples were washed in PBS (3x30'), incubated in SBT (2 hours at 4ºC) and incubated in QH1 primary antibody (1/100 diluted, DSHB) overnight at 4ºC. Samples were washed in PBS (3x30') and incubated in Cy5 AffiniPure Donkey Anti-Mouse IgG (1/200 diluted, Jackson 715-175-150) and DAPI (1/2000 diluted, Sigma D9542) for 5 hours at 4ºC. Finally, the samples were washed in PBS (3x30') before analysis under a LEICA SP5 laser confocal microscope. All the incubations were done on an orbital shaker.

In situ hybridization

In situ hybridization was performed as previously described (Kruithof et al., 2006). The embryos were sectioned at 10μm, deparaffinized, rehydrated in a graded series of alcohol and incubated with 10mg/ml proteinase K dissolved in PBS for 15min at 37ºC. The proteinase K activity was blocked by rinsing the sections in 0.2% glycinein PBST (PBS + 0.05%Tween-20) for 5min. After rinsing in PBS, the sections were post-fixed for 10 min in 4% PFA and 0.2% glutaraldehyde in PBS, followed by rinsing in PBS. After pre-hybridization for at least 1h at 70ºC in hybridization mix: 50%formamide, 5 X SSC (20 X SSC, 3M NaCl, 0.3M tri-sodium citrate, pH4.5),1% blocking solution (Roche), 5mM EDTA, 0.1% 3-[(3-cholamidopropyl) dimethylammonio]-1-pro panesulfonate (SIGMA), 0.5mg/ml heparin (BD Biosciences), and 1mg/ml yeast total RNA (Roche),digoxigenin(DIG)-labeled EphrinB2 or Notch1 probe was added to the hybridization mix to a final concentration of 1ng/ml.

Acknowledgments

The authors thank Dr. Isabel Palmeirim and Dr. Yoshiko Takahashi for the avian Notch1 and EphrinB2 riboprobes, respectively and Dr. Rita Carmona for her help with *in situ* hibridization. The TG-bound VEGF fibrin matrix was a kind gift from the late Dr. A. Zisch.

References:

Ando K, Nakajima Y, Yamagishi T, Yamamoto S, Nakamura H. 2004. Development of Proximal Coronary Arteries in Quail Embryonic Heart: Multiple Capillaries Penetrating the Aortic Sinus Fuse to Form Main Coronary Trunk. Circ Res 94:346–352.

Bogers A, Gittenberger-de Groot AC, Poelmann R, Péault B, Huysmans H. 1989. Development of the origin of the coronary arteries, a matter of ingrowth or outgrowth? Anat Embryol 180:437–441.

Cano E, Carmona R, Ruiz-Villalba A, Rojas A, Chau Y-Y, Wagner KD, Wagner N, Hastie ND, Muñoz-Chápuli R, Pérez-Pomares JM. 2016. Extracardiac septum transversum/proepicardial endothelial cells pattern embryonic coronary arterio-venous connections. Proc Natl Acad Sci USA 113:656–661.

Conte G, Pellegrini A. 1984. On the development of the coronary arteries in human embryos, stages 14-19. Anat Embryol 169:209–218.

Dettman RW, Denetclaw W, Ordahl CP, Bristow J. 1998. Common Epicardial Origin of Coronary Vascular Smooth Muscle, Perivascular Fibroblasts, and Intermyocardial Fibroblasts in the Avian Heart. Dev Biol 193:169–181.

Drake CJ, Brandt SJ, Trusk TC, Little CD. 1997. TAL1/SCL is expressed in endothelial progenitor cells/angioblasts and defines a dorsal-to-ventral gradient of vasculogenesis. Dev Biol 192:17–30.

Drake CJ, Fleming PA. 2000. Vasculogenesis in the day 6.5 to 9.5 mouse embryo. Blood 95:1671–1679.

Flamme I, Breier G, Risau W. 1995. Vascular endothelial growth factor (VEGF) and VEGF receptor 2 (flk-1) are expressed during vasculogenesis and vascular differentiation in the quail embryo. Dev Biol 169:699–712.

Grego-Bessa J, Luna-Zurita L, del Monte G, Bolós V, Melgar P, Arandilla A, Garratt AN, Zang H, Mukouyama YS, Chen H, Shou W, Ballestar E, Esteller M, Rojas A, Pérez-Pomares JM, de la Pompa JL. 2007. Notch Signaling Is Essential for Ventricular Chamber Development. Dev Cell 12:415–429.

Guadix JA, Carmona R, Muñoz-Chápuli R, Pérez-Pomares JM. 2006. In vivo and in vitro analysis of the vasculogenic potential of avian proepicardial and epicardial cells. Dev Dyn 235:1014–1026.

Hamburger V, Hamilton HL. 1951. A series of normal stages in the development of the chick embryo. J Morphol 88:49–92.

Hirakow R. 1983. Development of the cardiac blood vessels in staged human embryos. Acta Anat 115:220–230.

Hutchins MG, Kessler-Hanna A, Moore GW. 1988. Development of the coronary arteries in the embryonic human heart. Circulation 77:1250–1257.

Ivins S, Chappell J, Vernay B, Suntharalingham J, Martineau A, Mohun TJ, Scambler PJ. 2015. The CXCL12/CXCR4 Axis Plays a Critical Role in Coronary Artery Development. Dev Cell 33:455–468.

Jilani SM, Murphy TJ, Thai SNM, Eichmann A, Alva JA, Iruela-Arispe ML. 2003. Selective binding of lectins to embryonic chicken vasculature. J Histochem Cytochem 51:597–604.

Kattan J, Dettman RW, Bristow J. 2004. Formation and Remodeling of the Coronary Vascular Bed the Embryonic Avian Heart. Dev Dyn 230:34–43.

Katz TC, Singh MK, Degenhardt K, Rivera-Feliciano J, Johnson RL, Epstein JA, Tabin CJ. 2012. Distinct Compartments of the Proepicardial Organ Give Rise to Coronary Vascular Endothelial Cells. Dev Cell 22:639–650.

Kelly RG, Brown NA, Buckingham ME. 2001. The Arterial Pole of the Mouse Heart Forms from Fgf10-Expressing Cells in Pharyngeal Mesoderm. Dev Cell 1:435–440.

Kruithof BPT, van Wijk B, Somi S, Kruithof-de Julio M, Pérez Pomares JM, Weesie F, Wessels A, Moorman AFM, van den Hoff MJB. 2006. BMP and FGF regulate the differentiation of multipotential pericardial mesoderm into the myocardial or epicardial lineage. Dev Biol 295:507–522.

Lavine KJ, Ornitz DM. 2008. Fibroblast growth factors and Hedgehogs: at the heart of the epicardial signaling center. Trends Genet 24:33–40.

Lewis F. 1904. The question of sinusoids. Anat Anz 25:261–279.

Liu H, Yang Q, Radhakrishnan K, Whitfield DE, Camille LM, Parsons-Wingerter P, Fisher SA. 2009. Role of VEGF and tissue hypoxia in patterning of neural and vascular cells recruited to the embryonic heart. Dev Dyn 238:2760–2769.

Luxán G, Casanova JC, Martínez-Poveda B, Prados B, D'Amato G, MacGrogan D, Gonzalez-Rajal A, Dobarro D, Torroja C, Martinez F, Izquierdo-García JL, Fernández-Friera L, Sabater-Molina M, Kong Y-Y, Pizarro G, Ibañez B, Medrano C, García-Pavía P, Gimeno JR, Monserrat L, Jiménez-Borreguero LJ, de la Pompa JL. 2013. Mutations in the NOTCH pathway regulator MIB1 cause left ventricular noncompaction cardiomyopathy. Nat Med 19:193–201.

Männer J. 1999. Does the subepicardial mesenchyme contribute myocardioblasts to the myocardium of the chick embryo heart? A quail-chick chimera study tracing the fate of the epicardial primordium. Anat Rec 255:212–226.

Mikawa T, Fischman DA. 1992. Retroviral analysis of cardiac morphogenesis: discontinuous formation of coronary vessels. Proc Natl Acad Sci USA 89:9504–9508.

Mikawa T, Gourdie RG. 1996. Pericardial mesoderm generates a population of coronary smooth muscle cells migrating into the heart along with ingrowth of the epicardial organ. Dev Biol 174:221–232.

Moyon D, Pardanaud L, Yuan L, Bréant C, Eichmann A. 2001. Plasticity of endothelial cells during arterial-venous differentiation in the avian embryo. Development 128:3359–3370.

Nesbitt T, Lemley A, Davis J, Yost MJ, Goodwin RL, Potts JD. 2006. Epicardial development in the rat: a new perspective. Microsc Microanal 12:390–398.

Le Noble F, Moyon D, Pardanaud L, Yuan L, Djonov V, Matthijsen R, Bréant C, Fleury V, Eichmann A, Le NF, Moyon D, Pardanaud L, Yuan L, Djonov V, Matthijsen R, Breant C, Fleury V, Eichmann A. 2004. Flow regulates arterial-venous differentiation in the chick embryo yolk sac. Development 131:361–375.

Pérez-Pomares JM, Macias D, Garcia-Garrido L, Munoz-Chapuli R. 1998. The origin of the subepicardial mesenchyme in the avian embryo: an immunohistochemical and quail-chick chimera study. Dev Biol 200:57–68.

Pérez-Pomares JM, Carmona R, González-Iriarte M, Atencia G, Wessels A, Muñoz-Chapuli R. 2002. Origin of coronary endothelial cells from epicardial mesothelium in avian embryos. Int J Dev Biol 46:1005–1013.

Pérez-Pomares JM, Phelps A, Sedmerova M, Carmona R, González-Iriarte M, Muñoz-Chápuli R, Wessels A. 2002. Experimental studies on the spatiotemporal expression of WT1 and RALDH2 in the embryonic avian heart: a model for the regulation of myocardial and valvuloseptal development by epicardially derived cells (EPDCs). Dev Biol 247:307–326.

Pérez-Pomares JM, De La Pompa JL, Franco D, Henderson D, Ho SY, Houyel L, Kelly RG, Sedmera D, Sheppard M, Sperling S, Thiene G, Van Den Hoff M, Basso C. 2016. Congenital coronary artery anomalies: A bridge from embryology to anatomy and pathophysiology-a position statement of the development, anatomy, and pathology ESC Working Group. Cardiovasc Res 109:204–216.

Pires-Gomes A, Pérez-Pomares JM. 2013. The Epicardium and Coronary Artery Formation. J Dev Biol 1:186–202.

Poelmann RE, Gittenberger-de Groot AC, Mentink MM, Bökenkamp R, Hogers B. 1993. Development of the cardiac coronary vascular endothelium, studied with antiendothelial antibodies, in chicken-quail chimeras. Circ Res 73:559–68.

Red-Horse K, Ueno H, Weissman IL, Krasnow MA. 2010. Coronary arteries form by developmental reprogramming of venous cells. Nature 464:549–553.

Ruiz-Villalba A, Ziogas A, Ehrbar M, Pérez-Pomares JM. 2013. Characterization of Epicardial-Derived Cardiac Interstitial Cells: Differentiation and Mobilization of Heart Fibroblast Progenitors. PLoS ONE 8:17–19.

Rychter Z, Oštádal B. 1971. Mechanism of the development of coronary arteries in chick embryo. Folia Morphol 19:113–124.

Steding G, Xu J, Seidl W, Männer J, Xia H. 1990. Developmental aspects of the sinus valves and the sinus venosus septum of the right atrium in human embryos. Anat Embryol 181:469–475.

Théveniau-Ruissy M, Pérez-Pomares JM, Parisot P, Baldini A, Miquerol L, Kelly RG. 2016. Coronary stem development in wild-type and Tbx1 null mouse hearts. Dev Dyn 245:445–459.

Tian X, Hu T, He L, Zhang H, Huang X, Poelmann RE, Liu W, Yang Z, Yan Y, Pu WT, Zhou B. 2013. Peritruncal coronary endothelial cells contribute to proximal coronary artery stems and their aortic orifices in the mouse heart. PLoS ONE 8:1–9.

Tian X, Pu WT, Zhou B. 2015. Cellular origin and developmental program of coronary angiogenesis. Circ Res 116:515–530.

Tomanek RJ, Christensen LP, Simons M, Murakami M, Zheng W, Schatteman GC. 2010. Embryonic coronary vasculogenesis and angiogenesis are regulated by interactions between multiple FGFs and VEGF and are influenced by mesenchymal stem cells. Dev Dyn 239:3182–3191.

Tomanek RJ, Hansen HK, Dedkov EI. 2006. Vascular patterning of the quail coronary system during development. Anat Rec 288:989–999.

Viragh S, Challice CE. 1981. The origin of the epicardium and the embryonic myocardial circulation in the mouse. Anat Rec 201:157–168.

Vrancken Peeters MP, Gittenberger-de Groot AC, Mentink MM, Hungerford JE, Little CD, Poelmann RE. 1997. Differences in development of coronary arteries and veins. Cardiovasc Res 36:101–110.

Vrancken Peeters MP, Gittenberger-de Groot AC, Mentink MM, Hungerford JE, Little CD, Poelmann RE. 1997. The development of the coronary vessels and their differentiation into arteries and veins in the embryonic quail heart. Developmental Dynamics, 208: 338-48.

Wagner N, Wagner KD, Theres H, Englert C, Schedl A, Scholz H. 2005. Coronary vessel development requires activation of the TrkB neurotrophin receptor by the Wilms' tumor transcription factor Wt1. Genes Dev 19:2631–2642.

Waldo K, Willner W, Kirby M. 1990. Origin of the proximal coronary artery stems and a review of ventricular vascularization in the chick embryo. Am J Anat 188:109–120.

Waldo KL, Kumiski DH, Wallis KT, Stadt HA, Hutson MR, Platt DH, Kirby ML. 2001. Conotruncal myocardium arises from a secondary heart field. Development 128:3179–3188.

Wu B, Zhang Z, Lui W, Chen X, Wang Y, Chamberlain AA, Moreno-Rodriguez RA, Markwald RR, O'Rourke BP, Sharp DJ, Zheng D, Lenz J, Baldwin HS, Chang CP, Zhou B. 2012.

Endocardial cells form the coronary arteries by angiogenesis through myocardial-endocardial VEGF signaling. Cell 151:1083–1096.

Zhang B, Pu WT. 2013. The mysterious origins of coronary vessels. Cell Res 23:1063–1064.

Zhang H, Pu W, Li G, Huang X, He L, Tian X, Liu Q, Zhang L, Wu SM, Sucov HM, Zhou B. 2016. Endocardium Minimally Contributes to Coronary Endothelium in the Embryonic Ventricular Free Walls. Circ Res 118:1880–1893.

Zhang Z, Zhou B. 2013. Accelerated Coronary Angiogenesis by Vegfr1-Knockout Endocardial Cells. PLoS ONE 8:1–11.

Zhou B, Pu WT. 2012. Genetic Cre-loxP assessment of epicardial cell fate using Wt1-Driven cre alleles. Circ Res 111:e276-e280.

Figure and table legends

Figure 1. ***Early avian coronary vasculature forms from sinus venosus endocardium and proepicardial (PE) angioblasts***. **A-C**. Quail embryos (HH17; HH21-23; HH28-29, respectively) were injected with FITC-conjugated *L. culinaris* lectin (LC-FITC) before fixation as shown. **D-E**. Before attaching to the myocardium (HH17), the PE contains $QH1^+$/$LC\text{-}FITC^-$ angioblasts (red, arrowheads). Both the sinus venosus and ventricular endocardium are $QH1^+$/$LC\text{-}FITC^+$ (yellow). **F-G**. At HH21 the primitive epicardium and subepicardial space are formed. **G-G'**. Sinus venosus endocardial sprouts (**G**, arrow, magnified in **G'**); only the tip-like cells in these sprouts remain $LC\text{-}FITC^-$ (G', arrow). **H**. At HH26, sinus venosus endocardial sprouts (arrow) growing into the subepicardial matrix are connected with the systemic circulation ($LC\text{-}FITC^+$); Subepicardial $QH1^+$/$LC\text{-}FITC^-$ angioblasts are also frequent (**G**, **H**, red, arrowheads). **I-L**. Transverse sections of HH23 hearts (**J-L**) show sinus venosus derivatives ($QH1^+$/$LC\text{-}FITC^+$, yellow, arrows) in the subepicardial space. **M-P**. Ventricular transverse sections illustrate the presence of both perfused subepicardial ($QH1^+$/$LC\text{-}FITC^+$, yellow, arrows) and non-perfused intramyocardial ($QH1^+$/$LC\text{-}FITC^-$, red, arrowheads) vascular structures in the ventricular wall from HH23. **Q-T.** At HH28-29 $QH1^+$/$LC\text{-}FITC^+$ (yellow, arrows) are mostly found in the myocardium; $QH1^+$/$LC\text{-}FITC^-$ vascular structures are intramyocardial (R, T, arrowheads). Cell nuclei were counterstained with DAPI (blue). **Abbreviations**: *AVC*: atrio-ventricular canal; *End*; endocardium; *Ep*: epicardium; *Li*: liver; *SE*: subepicardium; *SV*: sinus venosus; *SVE*; sinus venosus endocardium; *V*: ventricle; *VM*; ventricular myocardium. **Scale bars**: A-G, H-T: 50 μm; G': 20μm.

Figure 2. ***Whole heart staining confirms early avian coronary vasculature is composed of two different endothelial networks***. **A-C**. HH23 quail heart, dorsal (**A-B**) and ventral (**C**) views. Blood-perfused $QH1^+$/$LC\text{-}FITC^+$ endocardial sprouts from the sinus venosus (large boxed area in **A**, magnified in **B**) grow over the dorsal ventricular wall, coinciding in space and time with non-perfused $QH1^+$/$LC\text{-}FITC^-$ vasculogenic chords (small boxed area in **A**, magnified in **A'**). $QH1^+$/$LC\text{-}FITC^+$ primitive coronary vessels (**B**, arrows) interact with $QH1^+$/$LC\text{-}FITC^-$ cells (**B**, arrowheads). At this stage, the ventral ventricular wall is poorly vascularized, but $QH1^+$/$LC\text{-}FITC^-$ angioblasts (arrowheads) and vascular cords (boxed area, magnified in **C'**) are conspicuous. **D-J**. HH28-29 quail heart, dorsal (**D-E**), ventral (**F**) and cranial (**G-J**) views. In the dorsal ventricular wall $QH1^+$/$LC\text{-}FITC^+$ blood vessels have extended from the base of the heart towards the cardiac apex. Note that some $QH1^+$/$LC\text{-}FITC^-$ vascular structures (arrowheads) also grow in the same direction. The boxed area in **D** is magnified in **E** to show the formation of small vascular shunts between perfused ($QH1^+$/$LC\text{-}FITC^+$) and non-perfused ($QH1^+$/$LC\text{-}FITC^-$) coronary blood vessels (**E**, arrowheads). In the ventral wall, $QH1^+$/$LC\text{-}FITC^+$ vessels grow laterally following the AV canal (**F**, arrows) while $QH1^+$/$LC\text{-}FITC^-$ peritruncal vascular structures extend to the ventricular walls (**F**, arrowheads). Cranial view shows dorsal and ventral developing coronary vessels are not connected. The small boxed area in **G** (magnified in **I**, **J**)

show dorsal vessels include perfused (arrows) and non-perfused (arrowheads) vascular segments. The ventral, peritruncal blood vessels at the base of the cardiac outflow tract (**G**, large boxed area, magnified in **H**) are mostly QH1^{+}/LC-FITC^{-} (**H**, arrowheads). **K-N**. Whole mount immunostainings of HH28-29 hearts show coronary blood vessel arrangement along the arterial pole of the heart (the dashed lines in **K** mark the levels shown in sections **L**-**N**). Note that the majority of these peritruncal and arterial pole vessels are not perfused by LC-FITC (red, arrowheads). Cell nuclei are counterstained with DAPI (blue). **Abbreviations**: *Ao*: Aorta; *CV*: coronary vein; *LA*: left atrium; *LAVC*: left atrioventricular canal; *LV*: left ventricle; *OFT*: outflow tract; *Pu*: pulmonary artery; *RA*: right atrium; *RAVC*: right atrioventricular channel; *RV*: right ventricle; *SV*: sinus venosus. **Scale bars**: **A**-**C**, **D**, **F**, **G**, **H**: 100 μm; **E**, **I, J**: 50 μm; **K**: 300 μm; **L-N**: 200 μm.

Figure 3. ***Proepicardial contribution to avian coronary development.*** **A-A''.** Quail-to-chick proepicardial chimeras were constructed (**A**) and intravascularly injected with LC-FITC at different developmental stages (**A'**, **A''**). In **B**-**G** the outer epicardial surface and the subepicardial-myocardial transition are indicated with dotted and dashed lines, respectively. **B-C.** Donor proepicardial derivatives (QH1^{+}) at the base of the heart (HH23-24) locate either on the outer surface of nascent QH1^{-}/LC-FITC^{+} host-derived coronary vessels (**B**, red, arrowheads) or have mixed with host endothelium to form subepicardial and intramyocardial blood-perfused (LC-FITC^{+}) chimeric vessels (**C**, yellow, arrows). **D**. Apical sections of HH23-24 chimeric ventricles show donor proepicardial-derived cells forming primitive vascular cords in the subepicardium (red, arrowheads); the compact ventricular myocardial is not vascularized. **E**. At HH26, most donor proepicardial-derived cells (QH1^{+}) locate subepicardially, forming blood-perfused (LC-FITC^{+}) coronary vessels (yellow, arrows). Some of these cells remain isolated forming vascular structures disconnected from systemic blood flow (red, arrowheads). **F-G**. At HH28-29, donor proepicardial-derived cells contribute to blood-perfused (QH1^{+}/LC-FITC^{+}, yellow, arrows) and non-perfused (QH1+/LC-FITC-, red, arrowheads) coronary vessels (the vessels marked with asterisks in **F** are magnified in **G**). **H-I'**. Whole mount stainings of HH28-29 quail-to-chick chimeras allow for the immediate identification of proepicardial endothelial derivative incorporation to developing coronary vessels. In **H** (ventral view) QH1^{+}/LC-FITC^{-} vessels are conspicuous in the ventricles and the aortic and pulmonary root (arrowheads). Note that no donor-derived endothelial cells are found distally to the truncus (dotted lines in H, H'). In **I** (dorsal view) prospective coronary veins (LC-FITC^{+}) are found connected to the sinus venosus; the boxed area in **I** is magnified in **I'** to show donor-derived cells (QH1+) in these vessels (arrowheads). **J-M'**. Arterial endothelial markers EphrinB2 and Notch1 are expressed in late (HH42) coronary arteries but not veins (**J**). Stage-matched chimeras (HH42) display donor proepicardial-derived cells (QH1^{+}, green) overlapping (**K'**, **L'**, **M'**) with the endothelium of right coronary artery stem (**i**, EphrinB2^{+} mRNA+, purple) and major arterial coronary vessels (**L'**, **M'**, Notch1^{+} mRNA+, purple). **Abbreviations**: *Ao*: aorta; *CA*: coronary artery; *CV*: coronary vein; *End*: endocardium; *Ep*: epicardium; *LA*: left atrium; *LV*: left ventricle; *Pu*: pulmonary artery; *RA*:

right atrium; *RCA*: right coronary artery; *RV*: right ventricle; *SV*: sinus venosus; *VM*: ventricular myocardium. **Scale bars**: **B**, **F**, **G**: 50 μm; **C**: 100 μm**; D**: 25 μm; **E**: 30 μm; **H**,**I**: 300 μm; **H'**, **I'**: 50 μm; **J**, **K**, **K'**, **L, L'**: 25 μm; **M**, **M'**: 15 μm.

Figure 4. ***Ventricular endocardium has the potential to contribute to coronary vessel formation.*** **A-N.** Quail-to-chick proepicardial (**A**) and ventricular chimeras (**H**) are compared. **B-G.** From HH23 (**B-D**) to HH28-29 (**E-G**) donor proepicardial-derived vascular cells ($QH1^+$, red, arrows) progressively vascularize the subepicardium and myocardium of ventricular walls. Lectin intravascular injections were used to counterstain the endocardium ($LC\text{-}FITC^+$, green, arrows). **I-N**. Early ventricular chimeras (**I-K**, HH23) show a fast incorporation of donor ventricular endocardium-derived vascular cells ($QH1^+$, red, arrowheads) to the host ventricular endocardium ($LC\text{-}FITC^+$, green, arrowheads). In late chimeras (**L-N**, HH28-29) donor ventricular endocardium-derived vascular cells also incorporate to the host endocardium ($QH1^+/LC\text{-}FITC^+$, yellow, arrowheads), but some of them remain in the compact ventricular myocardium forming vascular structures that are disconnected from the blood flow ($QH1^+/LC\text{-}FITC^-$, red, arrowheads). The boxed area in **L-N** has been magnified to show these structures in detail. **Abbreviations**: *CVM*: compact ventricular myocardium; *End*: endocardium; *Ep*: epicardium. **Scale bars**: 50 μm.

Figure 5. Distal cardiac outflow tract (OFT) endothelial cells contribute to coronary vascular development. A. To test the potential contribution of distal cardiac OFT endothelial cells (boxed area in **A**, left) to coronary vascularization, DiO and homotopic quail-to-chick transplantations (**A**, middle) were performed and cells were tracked as indicated (**A**, right). **B-H''.** Control DiO stainings of the distal cardiac OFT show the stain is originally restricted to this area (**B**, **C**, arrows). After 48 hours DiO tagged cells concentrate at the proximal cardiac outflow tract (**D**, green, arrowheads). Tissue sections confirm this staining pattern (compare **E** with **F-H''**). Endothelial cells (VEGFR2+, red) close to the aortic sac (**G**, arrowheads) are in continuity with DiO^+ (green) endothelial cells (VEGFR2+, red) of the OFT walls (**H**-**H**'', arrowheads). The region of the heart shown in J-L is boxed in **I**. **J.** The peritruncal capillary plexus is patent at stages HH32-33. **K-L.** Cardiac distal outflow tract-derived endothelial cell incorporation to the forming peritruncal plexus was tracked using distal cardiac outflow tract homotopic quail-to-chick transplantations (see also **A**, middle). Donor-derived QH1+ endothelial cells (green) incorporate to the aortic root, just at the level of the forming ventriculo-arterial valves (**K**, arrowheads). Some of these cells penetrate the valvular walls (**L**, arrowheads). **M.** A model for the integration of different coronary endothelial cell populations is shown. **Abbreviations**: *A*: atrium; *Ao*: aorta; *dOFT*: distal cardiac outflow tract; *LA*: left atrium; *LV*: left ventricle; *OFT*: cardiac outflow tract; PE: proepicardium; *Pu*: pulmonary artery; *RA*: right atrium; *RV*: right ventricle; *SV*: sinus venosus; *V:* ventricle; **Scale bars**: **B**: 500 μm; **C**: 100 μm; **d**: 50 μm; **E**, **F**: 100 μm; **G**, **H**, **H'**, **H''**: 35 μm; **J**: 200 μm; **K**:100 μm; **L**: 20 μm.

Table 1. Endothelial cells from different sources contribute to distinct domains of the developing coronary vascular tree. Endothelial cell contribution to developing coronary vessels is indicated (+) for each transplantation method. In all cases, blood vessels are identified as connected to or disconnected from the systemic circulation by their staining after *Lens culinaris*-FITC intravascular injection (LC-FITC+ and LC-FITC-, respectively).

Table 1

Method	Donor endothelial cells ($QH1^+$) in vessels connected to the systemic flow (LC-FITC+)	Donor endothelial cells ($QH1^+$) in vessels disconnected to the systemic flow (LC-FITC-)	Donor endothelial cells ($QH1^+$) in the endocardium (LC-FITC+)
Quail proepicardial chimeras	+	+	-
Quail ventricular chimeras	+	+	+
Quail distal cardiac outflow tract chimeras	-	+	-

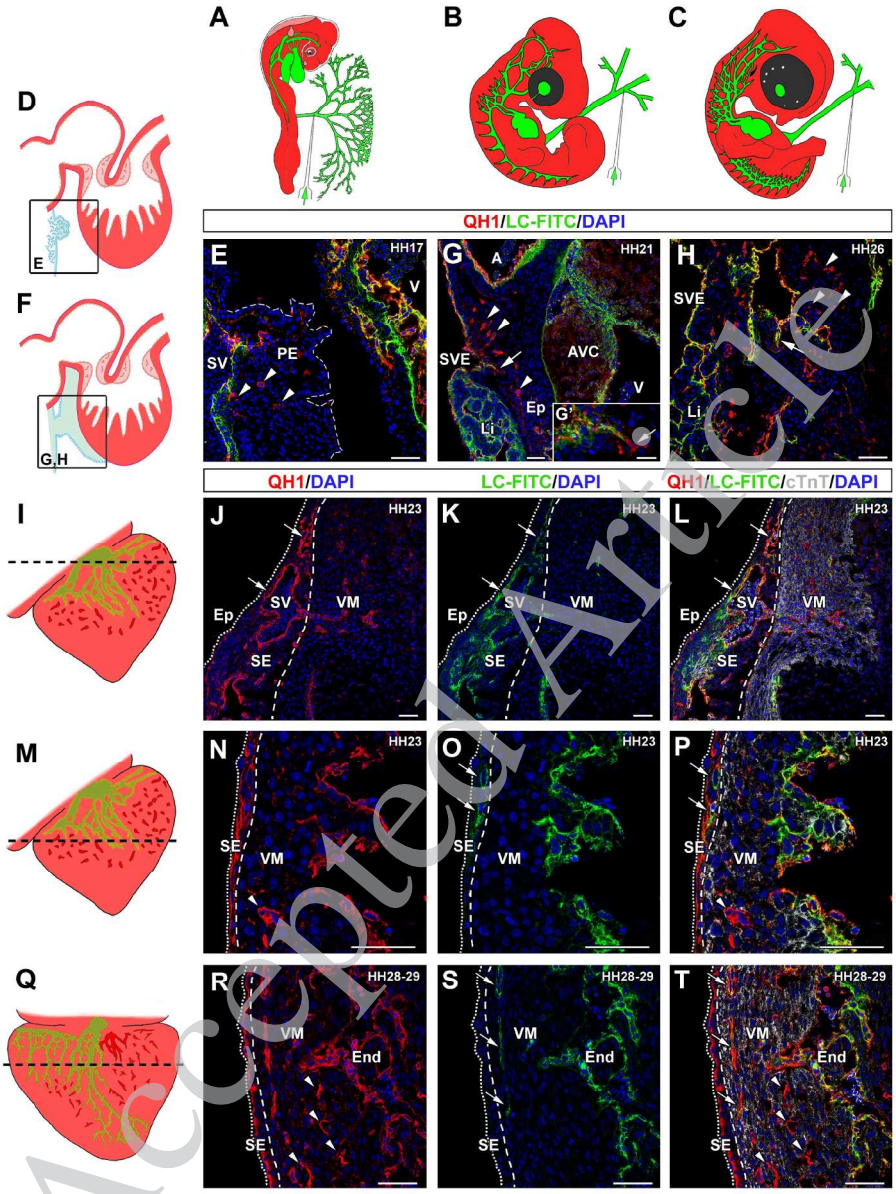

Figure 1

226x294mm (300 x 300 DPI)

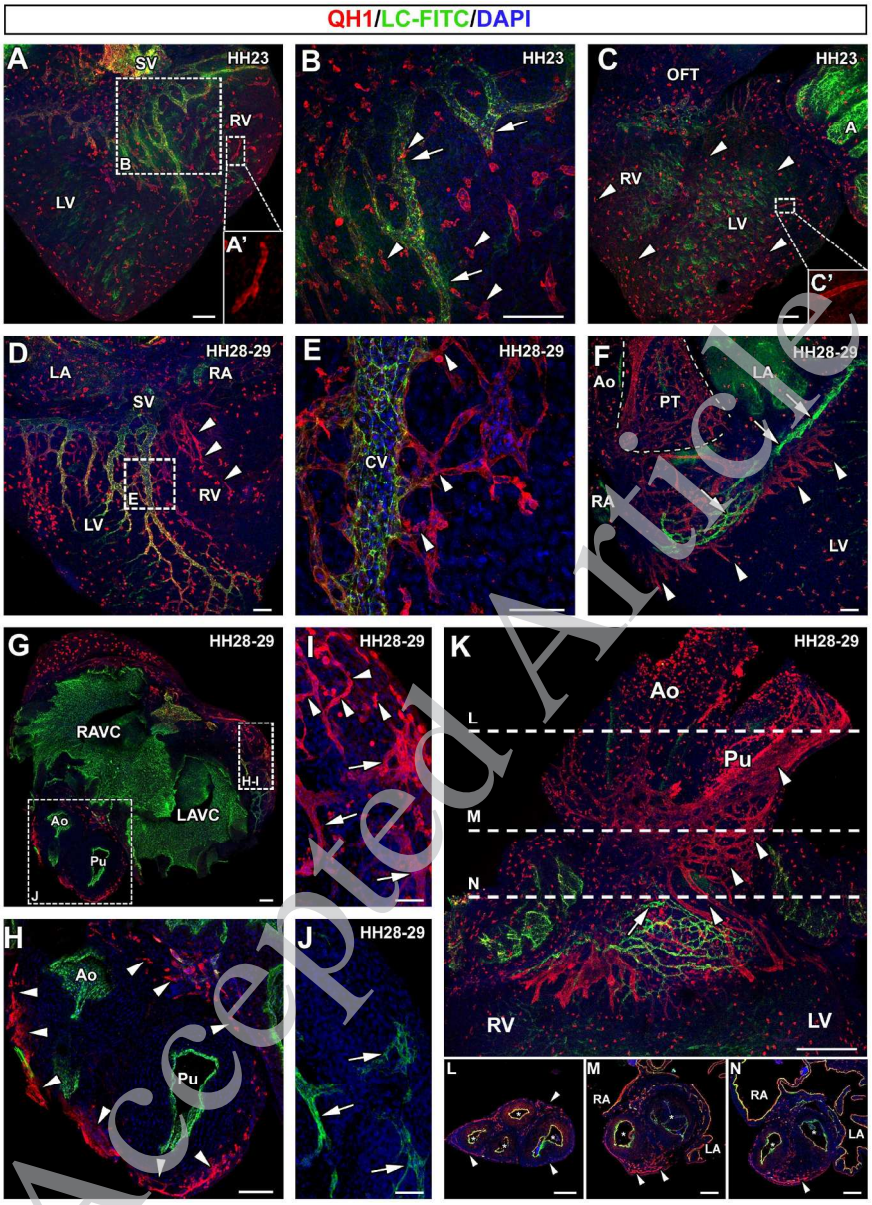

Figure 2

226x312mm (300 x 300 DPI)

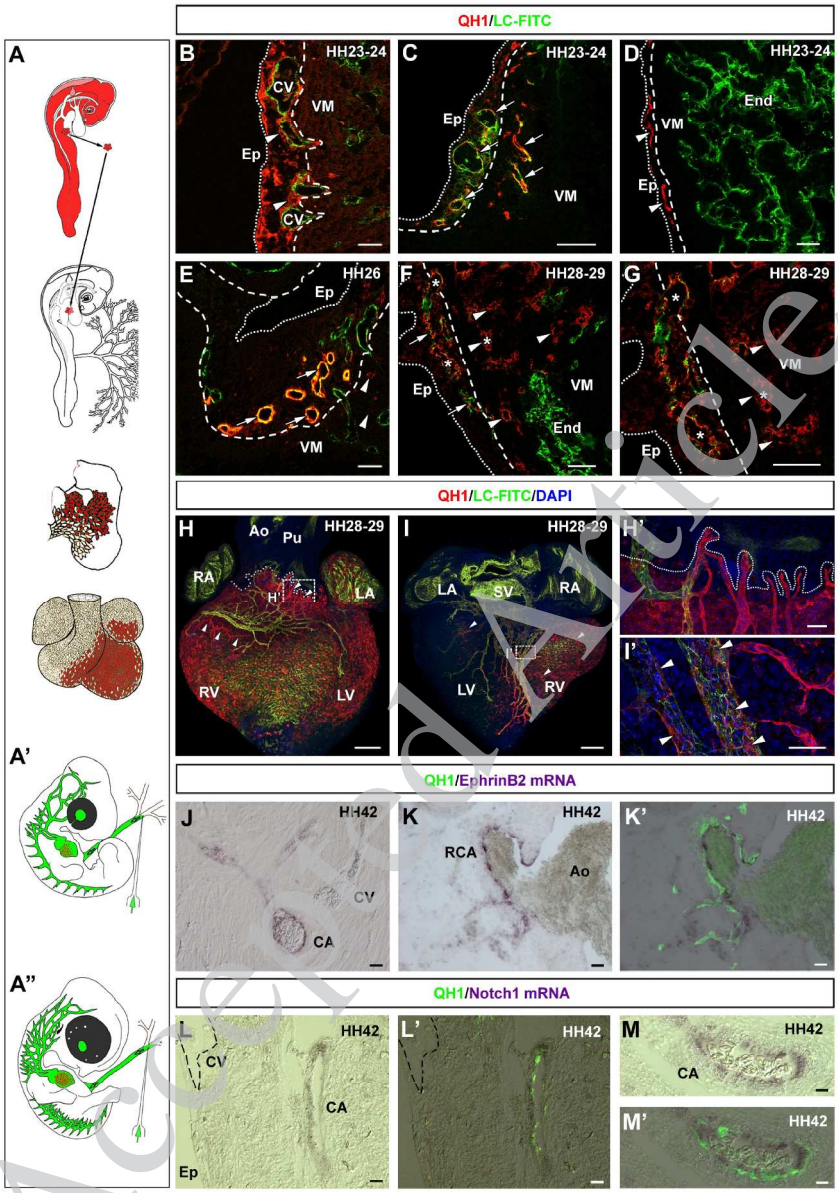

Figure 3

226x324mm (300 x 300 DPI)

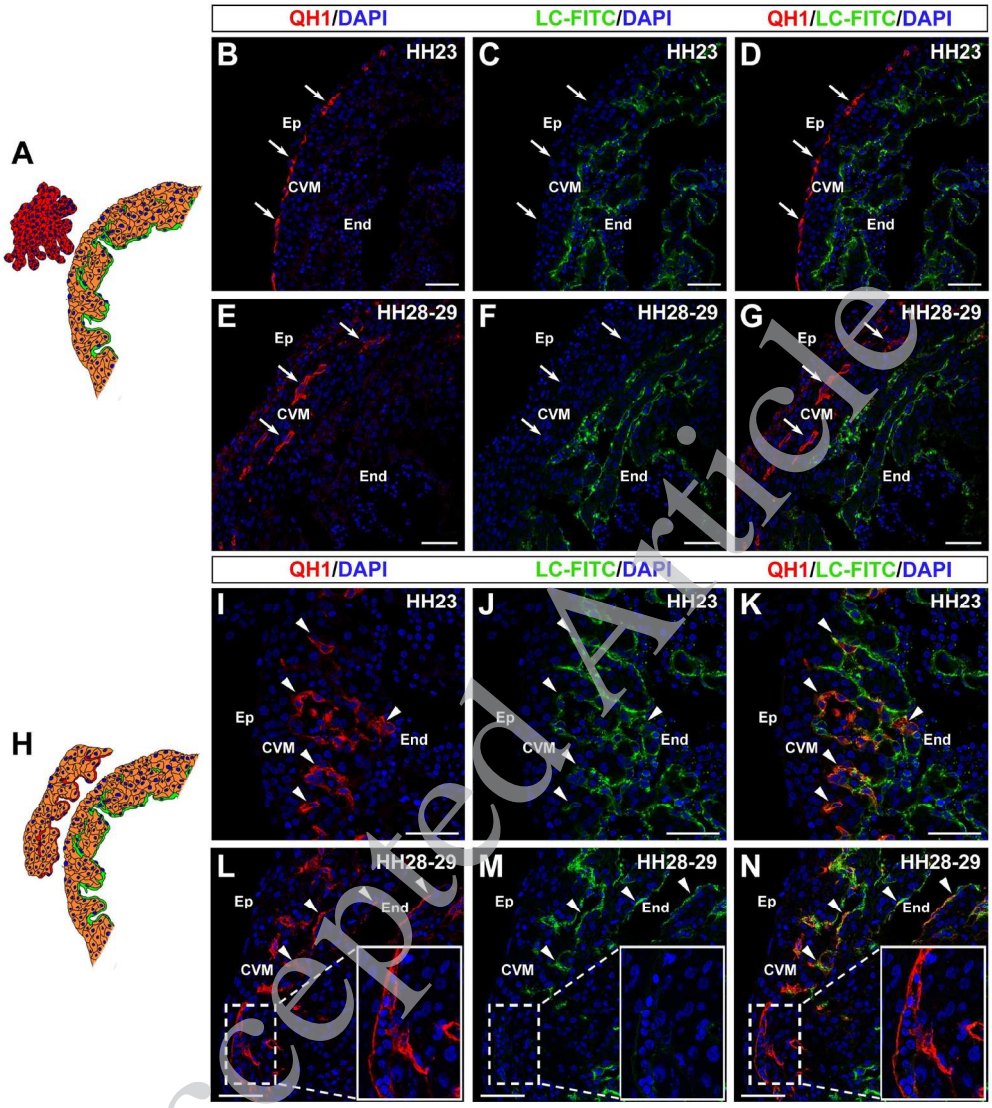

Figure 4

194x217mm (300 x 300 DPI)

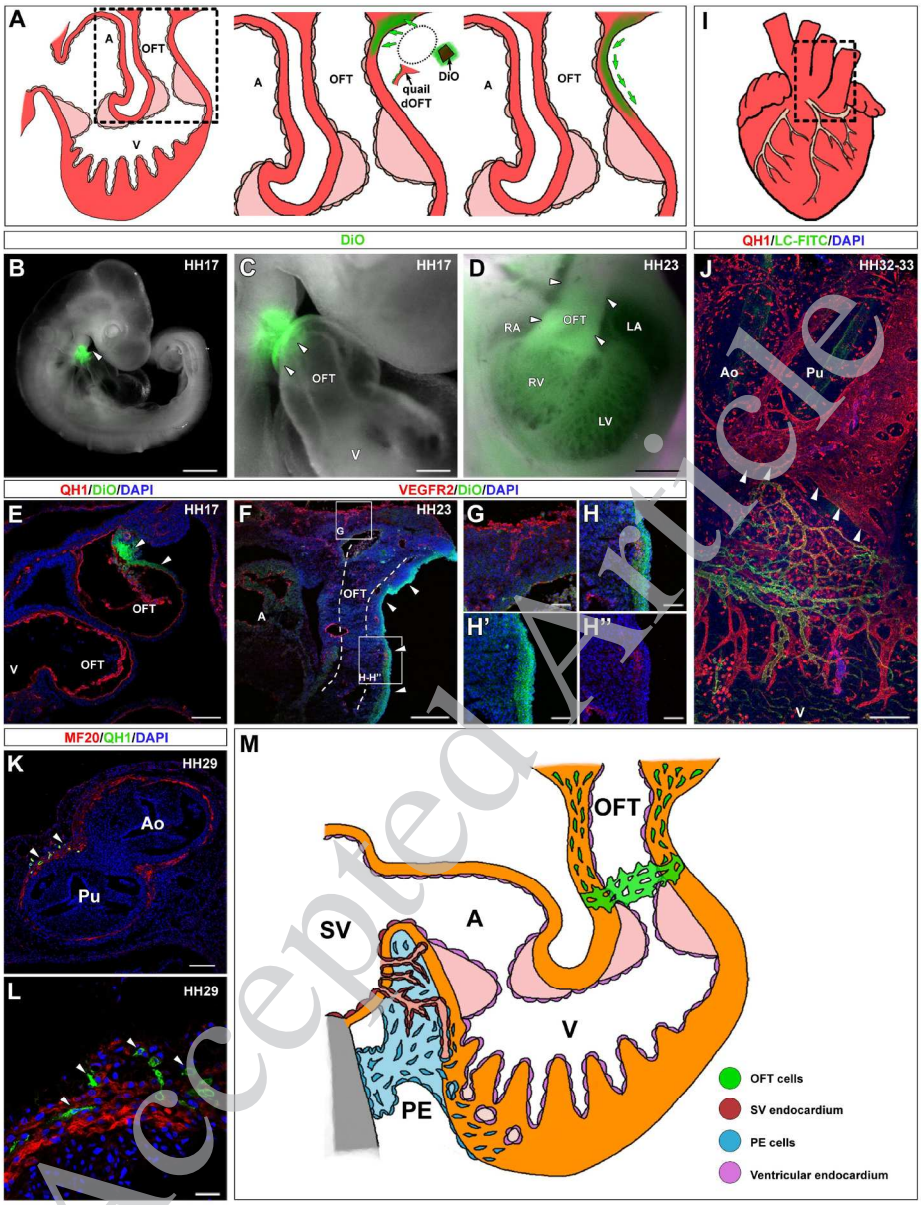

Figure 5

226x294mm (300 x 300 DPI)